Catalytic Materials

DOI: 10.1002/ange.201309660

Tunable Oxygen Activation for Catalytic Organic Oxidation: Schottky Junction versus Plasmonic Effects**

Ran Long, Keke Mao, Ming Gong, Shan Zhou, Jiahua Hu, Min Zhi, Yang You, Song Bai, Jun Jiang, Qun Zhang, Xiaojun Wu,* and Yujie Xiong**

Abstract: *The charge state of the Pd surface is a critical parameter in terms of the ability of Pd nanocrystals to activate O_2 to generate a species that behaves like singlet O_2 both chemically and physically. Motivated by this finding, we designed a metal–semiconductor hybrid system in which Pd nanocrystals enclosed by {100} facets are deposited on TiO_2 supports. Driven by the Schottky junction, the TiO_2 supports can provide electrons for metal catalysts under illumination by appropriate light. Further examination by ultrafast spectroscopy revealed that the plasmonics of Pd may force a large number of electrons to undergo reverse migration from Pd to the conduction band of TiO_2 under strong illumination, thus lowering the electron density of the Pd surface as a side effect. We were therefore able to rationally tailor the charge state of the metal surface and thus modulate the function of Pd nanocrystals in O_2 activation and organic oxidation reactions by simply altering the intensity of light shed on Pd–TiO_2 hybrid structures.*

The activation of molecular oxygen (O_2) is a critical step in various oxidation reactions, including epoxidation[1] and oxidations of CO,[2] hydrocarbons,[3] alcohols,[4] and glucose.[5] In the oxidation reactions, singlet oxygen is a highly reactive species in contrast to the inert ground state of O_2.[6] However, the excitation of triplet to singlet O_2 requires a spin-flip process that remains challenging, and is mainly limited by the spin selection rule.[7] In recent years, it has been reported that singlet O_2 can be generated with metal nanoparticles.[8] This progress renders metal nanoparticles very promising and versatile catalysts in various organic oxidation reactions.[8] Most recently, we revealed that the chemisorption of O_2 on Pd nanocrystals induces a spin reduction in O_2 that is mainly caused by electron transfer from the Pd surface to the O_2 antibonding π^* orbital.[9] Better than other facets, such as Pd {111}, Pd {100} can reduce the magnetic moment of O_2 to nearly zero;[9] as a direct outcome, the adsorbed O_2 species exhibits similar chemical and physical properties to singlet O_2 without the need for spin flipping.

Since the Pd→O_2 electron transfer is responsible for O_2 activation, the charge state of the metal surface may offer a handle for tuning its efficiency, which is fundamentally important to the optimization of catalyst design for organic oxidation. It is known that the electron density of a single metal should be constant, so it is imperative to introduce an additional electron source into the Pd system for the purpose of tailoring its charge state. The concept of the metal–semiconductor (M–S) configuration for photocatalysis gives us some clues.[10] In a process driven by the Schottky barrier, Pt cocatalysts can extract the photoexcited electrons from an n-type semiconductor, such as TiO_2, and serve as reduction sites for H_2 production in water splitting.[11] This widely used design for photocatalysis indicated to us that the charge of the Pd surface may be tailored by the M–S junction to tune the O_2 activation. This strategy is intuitively straightforward, and its feasibility has been exhibited in hydrogenation reactions. In hydrogenation reactions, H_2 activation can be maneuvered through variations in the electronic structure of metal catalysts supported on semiconductors.[12] Nevertheless, the carrier dynamics in the M–S junction are so complicated that the O_2-activation efficacy of this design cannot be warranted. For example, in parallel to the aforementioned electron transfer, the surface plasmon band of the metal may be excited under illumination to generate hot electrons.[13–15] A significant fraction of the plasmonic hot electrons should be energetic enough to reach the M–S interface and enter the conduction band of the semiconductor in a process that competes with the Schottky junction driven electron transfer.

Herein, we demonstrate by the use of Pd–TiO_2 hybrid structures as a proof-of-concept model that this injection of plasmonic hot electrons into TiO_2 may lower the electron density of the Pd surface in opposition to the function of the Schottky junction. By varying the illumination intensity, it is feasible to modulate the charge state of the Pd surface in this M–S hybrid configuration. Such modulation enables optimization of O_2 activation and in turn improvement of the

[*] R. Long,[+] K. Mao,[+] M. Gong, S. Zhou, J. Hu, M. Zhi, Y. You, S. Bai, Prof. J. Jiang, Prof. Q. Zhang, Prof. X. Wu, Prof. Y. Xiong
Hefei National Laboratory for Physical Sciences at the Microscale
Collaborative Innovation Center of Chemistry for Energy Materials
School of Chemistry and Materials Science
CAS Key Laboratory of Materials for Energy Conversion and
Laboratory of Engineering and Material Science
University of Science and Technology of China
Hefei, Anhui 230026 (P.R. China)
E-mail: qunzh@ustc.edu.cn
xjwu@ustc.edu.cn
yjxiong@ustc.edu.cn
Homepage: http://staff.ustc.edu.cn/~yjxiong/

[+] These authors contributed equally.

[**] This research was financially supported by the 973 Program (Nos. 2014CB848900, 2011CB921400, 2012CB922001, 2010CB923300), the NSFC (Nos. 21101145, 21121003, 51172223, 91127042, 21173205), the Recruitment Program of Global Experts, the CAS Hundred Talent Program, CAS Strategic Priority Research Program B (No. XDB01020000), and the Fundamental Research Funds for the Central Universities (No. WK2060190025, WK2060140014). We are grateful to Prof. Yi Luo for helpful discussions.

Supporting information for this article is available on the WWW under http://dx.doi.org/10.1002/anie.201309660.

efficiency of catalytic glucose oxidation by shedding appropriate light on the Pd–TiO_2 hybrid structures.

We first synthesized Pd–TiO_2 hybrid structures with exposed Pd {100} facets, which allow electron transfer between Pd and TiO_2, through a protocol modified from that described previously.[16] To evaluate the efficacy of the M–S junction, we used bare Pd nanocubes with {100} facets as a reference catalyst in the characterization of active O_2 species and glucose-oxidation tests. Transmission electron microscopy (TEM) images (Figure 1a and Figure S1a in the Supporting Information) clearly showed that the Pd nanocrystals in both samples had a cubic profile with an average edge length of 14 nm. High-resolution TEM (HRTEM) images (Figure 1b and Figure S1b) of the nanocrystals in the corresponding samples showed that the nanocubes were enclosed by well-defined {100} facets in both samples. As the two samples were identical in terms of Pd surface facets and size, we can safely rule out the possibility that the O_2 activation is affected by shape or size effects in the following catalysis tests. The only difference between the samples is the presence or absence of a semiconductor support, which can alter the charge state of Pd through charge transfer under illumination. The compositions and phases were characterized by energy-dispersive spectroscopy (EDS; see Figure S2) and X-ray diffraction (XRD; see Figure S3).

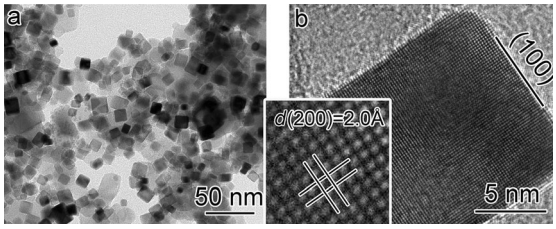

Figure 1. a) TEM and b) HRTEM images of Pd–TiO_2 hybrid structures. The inset in (b) is a magnified image showing the lattice fringes of Pd.

Following the successful synthesis of Pd–TiO_2 hybrid structures with well-defined Pd facets, we investigated their performance in O_2 activation. It is known that singlet O_2 species can be trapped by 2,2,6,6-tetramethyl-4-piperidone (4-oxo-TMP) to produce the stable nitroxide radical 4-oxo-TEMPO; thus, 4-oxo-TMP can be used as a probe molecule for the detection of singlet O_2.[17] Figure 2a shows the electron spin resonance (ESR) spectra of the samples obtained by mixing 4-oxo-TMP with the Pd nanocubes or the Pd–TiO_2 hybrid structures under UV illumination. The signals are consistent with those documented for 4-oxo-TEMPO[17] and thus suggest that a species that behaves chemically like singlet O_2 is formed upon the addition of the samples. Although both samples promoted the formation of 4-oxo-TEMPO, the intensity of the 4-oxo-TEMPO signals was stronger with the Pd–TiO_2 hybrid structures than with bare Pd. Measurements performed with a control sample, TiO_2, indicated that TiO_2 alone cannot generate a significant amount of the activated oxygen species. The formation of a species analogous to singlet O_2 in our system was also confirmed by a control

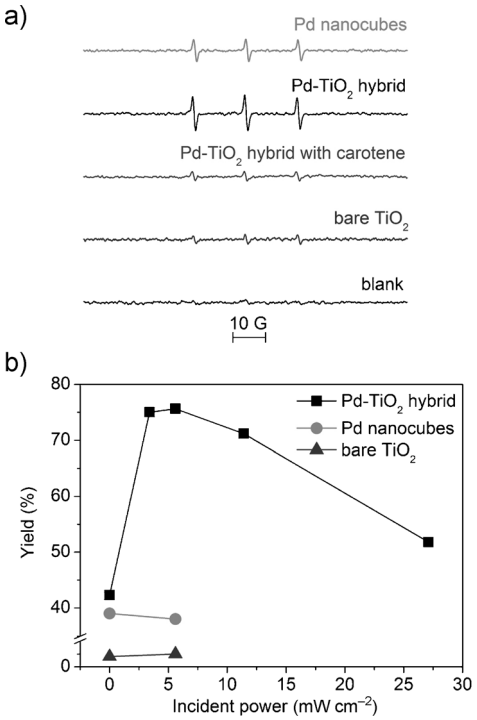

Figure 2. a) ESR spectra of the samples formed by mixing a solution of 4-oxo-TMP with Pd nanocubes, Pd–TiO_2 hybrid structures, and bare TiO_2. The spectrum of the Pd–TiO_2 hybrid structures in the presence of the singlet-O_2 scavenger carotene is also shown. A background curve was collected for the 4-oxo-TMP solution as a reference. b) Plots showing the yield of gluconic acid ($t = 2$ h) versus the power intensity of incident UV light with Pd–TiO_2 hybrid structures as catalysts. Pd nanocubes and bare TiO_2 were used as reference samples. The plots are based on the data in Table S1 of the Supporting Information. Glucose: 15 mM; $catalyst_{surface}$: 0.8 ‰. Note that no by-products, such as fructose, 2-deoxy-D-glucose, and D-glucuronic acid, were observed.[23–25]

experiment in the presence of carotene, a typical scavenger for the elimination of singlet O_2.[18] This experiment clearly demonstrated that the signal of 4-oxo-TEMPO can be quenched by carotene in the case of Pd–TiO_2, thus suggesting that the species that appears in our system has the chemical characteristics of singlet O_2 indeed. This set of ESR measurements reveals that the ability of Pd nanocubes to activate O_2 can be tuned by integrating them with semiconductor supports under UV illumination.

The enhancement of O_2 activation on TiO_2-supported Pd nanocubes can be understood from the viewpoint of charge transfer. Under UV illumination, the Schottky barrier drives the transfer of the photoexcited electrons in TiO_2 to Pd,[10,11] thus increasing the electron density of the Pd surface. First-principles calculations revealed charge-dependent O_2-activation behavior on Pd nanocubes (see Figure S4). They suggest that both the O_2 magnetic moment and the O–O distance strongly correlate with the charge density of the Pd surface, because electron transfer from the Pd(100) surface to the antibonding π^* orbital of O_2 (about 0.7 electrons) is mainly responsible for the decrease in magnetism during chemisorption.[9] Appropriate quantities of additional electrons brought to the Pd surface will promote its activity in O_2 activation.

Note that the O_2-activation process in our case differs from other processes, such as the dissociation of O_2 molecules over a metal surface, which has been widely investigated.[19–21]

The light intensity, which affects the amount of electrons supplied to the Pd surface, therefore holds the key to modulating the efficiency of O_2 activation. Thus, stronger UV illumination on TiO_2 should induce the delivery of more electrons to the Pd surface and further promote the generation of singlet-O_2-analogous species. However, this feature cannot be well resolved by the ESR technique with the 4-oxo-TMP system, because the product 4-oxo-TEMPO is very sensitive to strong UV light, particularly in the presence of TiO_2 (see Figure S5). This limitation makes it unfeasible to systematically investigate the role of UV light (which is exactly the excitation spectral region for TiO_2) in O_2 activation. Nevertheless, the illumination effect can be examined for catalytic glucose oxidation instead.

Their different activity in generating singlet-O_2-analogous species enabled us to further evaluate the performance of Pd nanocubes and Pd–TiO_2 hybrid structures in catalyzing glucose oxidation.[22] As shown in Figure 2b, both samples can catalyze the oxidation of glucose, albeit with varying efficiency. To clarify the role of O_2 species in the reaction, we performed the glucose oxidation with Pd–TiO_2 in the presence of carotene (20 mg). The yield of gluconic acid after 2 h was 0% in the dark and only 1% under illumination. The results clearly show that the generation of singlet-O_2-analogous species is a vital step in the glucose oxidation catalyzed by palladium-based solid catalysts.[9]

In line with the ESR measurements, the catalytic efficiency of Pd–TiO_2 hybrid structures in the glucose oxidation under illumination was much higher than that of bare Pd nanocubes. At a surface-atom percentage of 0.8‰, the yield and turnover number (TON) with the Pd–TiO_2 hybrid structures reached 76% and 920, respectively, under illumination at 5.6 mW cm^{-2}. In sharp contrast, the corresponding values for the use of bare Pd nanocubes were only 37% and 449, respectively. As demonstrated in our previous study,[9] the yield for glucose oxidation cannot be enhanced by UV light in the case of Pd nanocubes. Thus, the significant yield enhancement by Pd–TiO_2 can be ascribed to the transfer of photoexcited electrons from TiO_2 to Pd as anticipated. This conclusion was further confirmed by the similarity of the yield with Pd–TiO_2 (42%) in the dark to that observed with Pd. TiO_2 alone has minimal catalytic activity, regardless of whether the reaction is performed in the dark or under UV light (see Table S1 in the Supporting Information). Certainly, the TON is highly dependent on the usage dose of the catalysts. For example, at a dose as low as 0.08‰, the TON of Pd–TiO_2 for the catalysis of glucose oxidation under illumination at 3.4 mW cm^{-2} can reach 5260, which is superior to that found for Pd nanocubes (see Table S2). As can be seen from the TEM images of the Pd–TiO_2 catalyst after glucose oxidation (see Figure S6), the morphology of the catalyst is well-maintained, thus suggesting that these catalysts can be recycled for long-term use.

Interestingly, the efficiency of Pd–TiO_2 in oxidizing glucose became lower when the UV intensity was further increased. For example, the yield of gluconic acid was reduced to 52% when incident light of 27.1 mW cm^{-2} was introduced into the reaction system. This feature indicates that the strong UV illumination diminishes the electron supply from TiO_2 to Pd. In fact, hot electrons can be generated on metal nanocrystals by the excitation of surface plasmons, which are in turn injected into the conduction band of the semiconductor at the M–S interface.[13–15] This plasmonic effect could generate a reverse flow of electrons from Pd to TiO_2 in our case, thus lowering the electron density of the Pd surface. To assess whether high-intensity illumination can induce this back flow, we used ultrafast spectroscopy to examine the dynamic electron behavior in our samples.

Ultrafast transient absorption (TA) spectroscopy provides a robust tool for tracking in real time the electron dynamics.[26] By using a femtosecond UV/Vis pump/white-light continuum (WLC) probe scheme (see the Supporting Information for details), we investigated the Pd–TiO_2 hybrid structures to analyze the transient electron behavior involved with reference to bare TiO_2 and Pd nanocubes. Two different pumping cases with center wavelengths at 480 and 350 nm, respectively, were examined. The 500–700 nm WLC probe yielded essentially the same TA features, and we therefore show herein a set of representative data taken at 520 nm (Figure 3). Under photoexcitation at 480 nm, bare TiO_2 produced no TA signal (Figure 3a), simply because its bandgap is larger than 3 eV (< 413 nm), whereas bare Pd exhibited the well-known plasmon-damping effect[27] in its TA kinetic trace (see the zoom-in initial window of 0–30 ps on the right-hand side of Figure 3a). Pd–TiO_2 exhibited a rather different dynamic behavior: Its recovery was much slower than that of bare Pd. This behavior can be understood as a result of hot-electron injection from Pd to TiO_2, followed by subsequent electron relaxation within the conduction band to yield the observed stimulated emission (SE) signal (with a negative value), which features a much slower recovery from the TiO_2 side (see Figure 3b). Note that the ground-state bleach (GSB) signal, which also has a negative value, is not responsible for this effect, as GSB should occur in a much bluer region reflecting the interband transition just across the bandgap of TiO_2. The SE signals observed in the spectral region of 500–700 nm provided by the WLC probe are consistent with the documented[28] as well as our measured photoluminescence (PL) spectra of bare TiO_2 (see Figure S7).

It is natural to wonder what would happen if both Pd and TiO_2 were excited in this hybrid system. Relevant typical data recorded with a 350 nm pump are shown in Figure 3c. Interestingly, no significant difference was found in the behavior of Pd–TiO_2 in the two cases. As depicted in Figure 3d, the 350 nm laser pulse (15 μJ pulse^{-1}) simultaneously excites Pd and TiO_2. Intuitively, two electron-transfer processes (with opposite directions) should occur under strong laser illumination, that is, the transfer of photoexcited electrons from TiO_2 to Pd driven by the n-type Schottky junction and the reverse injection of Pd hot electrons into the TiO_2 conduction band as a result of the plasmonic effect. The former process may give rise to a positive excited-state absorption (ESA) signal on the Pd side. However, no pronounced ESA signal was observed; instead, the aforementioned SE signal that originates from the latter process

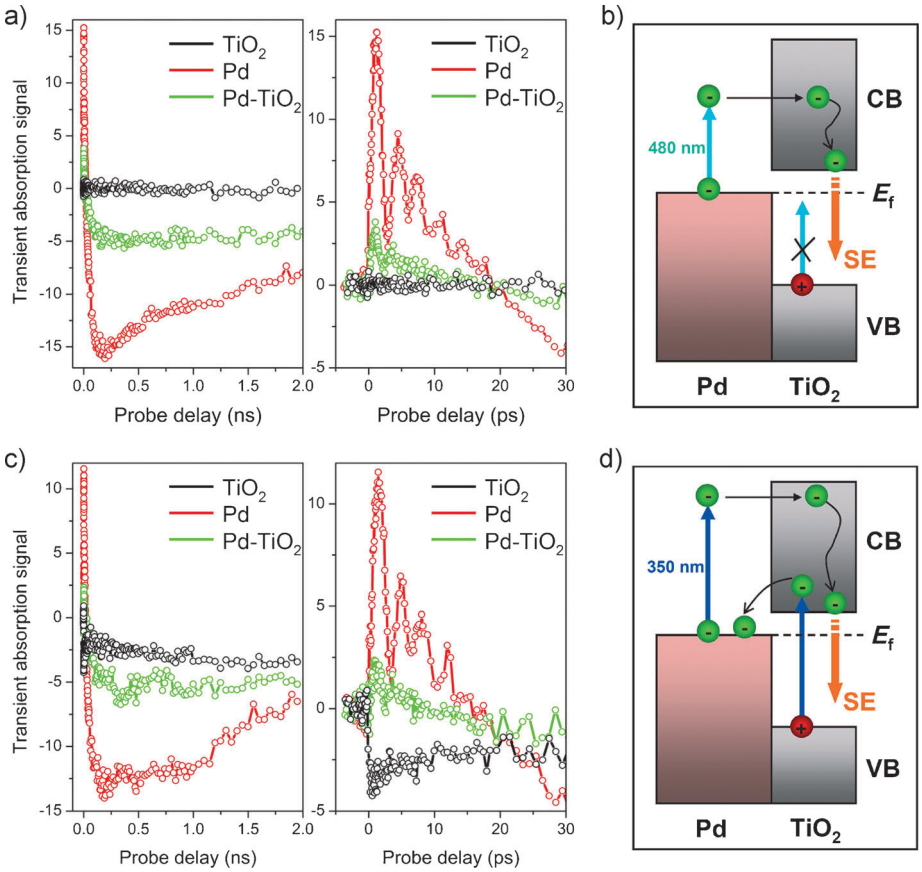

Figure 3. Ultrafast transient absorption (probed at 520 nm) as a function of probe delay for bare TiO_2, bare Pd nanocubes, and Pd–TiO_2 hybrid structures. a) Data recorded with a 480 nm pump (left: 0–2 ns; right: 0–30 ps). b) Schematic illustration of the electron behavior under photoexcitation at 480 nm. c) Data recorded with a 350 nm pump (left: 0–2 ns; right: 0–30 ps). d) Schematic illustration of the electron behavior under photoexcitation at 350 nm. VB, valence band; CB, conduction band; E_f, Fermi level; SE, stimulated emission.

still dominated. Nevertheless, the fluctuation during the recovery of the SE signal could be indicative of the involvement of such an ESA process. As a reference, the transient kinetics of bare TiO_2 are also shown in Figure 3c. In this case, there is apparent competition between SE and ESA, with the initial buildup and the subsequent decay features of ESA superimposed on the predominant SE trace. In the hybrid Pd–TiO_2 system of interest, the SE process induced by Pd hot electrons on the TiO_2 side is so strong as to completely suppress the ESA processes on both the Pd and TiO_2 sides (not depicted in Figure 3b,d). Note that bare Pd exhibits the plasmon-damping effect in its kinetic trace when pumped at 350 nm, similarly to when it is pumped at 480 nm, thus indicating the activation of Pd.[27]

It is well-known that Pd is a metal with relatively small plasmonic cross-sections, so its weak surface plasmon response can most likely be activated by high-intensity illumination.[27,29] It is safe to infer that the transfer of electrons from TiO_2 to Pd dominates when the illumination is relatively weak, thus promoting O_2 activation, as discussed above; however, its efficiency may be reduced by the plasmonic effect when the Pd nanocrystals are activated under strong illumination, as demonstrated in this study by ultrafast pump–probe measurements. Lowering of the pump pulse energy to 7 μJ pulse^{-1} and even to 3 μJ pulse^{-1} (close to our pump–probe detection limit) yielded similar TA kinetic profiles to the use of a pump pulse energy of 15 μJ pulse^{-1} (see Figure S8). This similarity is understandable because the peak power of the pump pulses in our pump–probe characterizations is rather high (given the pulse duration on the femtosecond timescale); such high-intensity illumination boosts the plasmonic effect so that only the plasmon-dominated electron-transfer process can be detected at different illumination wavelengths (i.e., 480 and 350 nm).

Nevertheless, the function of the Schottky junction can be well resolved by photocurrent measurements (Figure 4; see also Figure S9). As compared with bare TiO_2, Pd–TiO_2 hybrid structures give greatly enhanced photocurrents at relatively low light intensity, thus indicating the improved charge separation in TiO_2 by the Schottky junction. When the light intensity is increased to the extreme, a reduction in photocurrent is observed for the Pd–TiO_2 hybrid structures, thus implying the reverse injection of hot electrons by the plasmonic effect of Pd.

In summary, we have developed a metal–semiconductor hybrid structure—Pd–TiO_2—whose Pd components possess a cubic shape comparable to {100}-enclosed Pd nanocubes

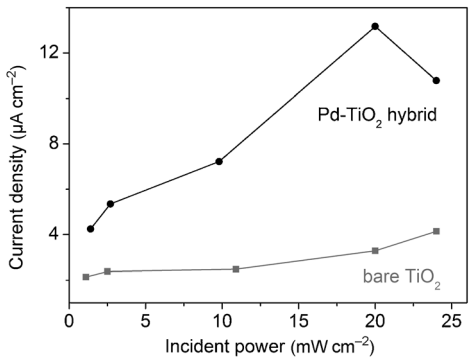

Figure 4. Transient photocurrent response of bare TiO_2 and Pd–TiO_2 hybrid structures at the same weight of TiO_2 when illuminated with light of varying intensity. Note that the incident power in this case (which reaches a maximum at about 24 mW cm^{-2}) is not comparable to that for glucose oxidation owing to very different experimental setups.

that are active for the production of singlet-O_2-analogous species. The success in the materials synthesis enables the design of nanomaterials with the same Pd surface facets but with very different electron states, as the semiconductor supports can supply electrons to the Pd surface under illumination as a result of the Schottky barrier. On the other hand, the Pd components can be activated by strong illumination to reversely inject hot electrons into the conduction band of TiO_2, thus lowering the electron density of the Pd surface. As O_2 activation is highly dependent on the charge state of the Pd surface, simple variation of the intensity of illumination on metal–semiconductor hybrid structures is a promising approach for tuning catalytic efficiency in organic oxidation reactions. It is anticipated that the new light cast by the present study on the importance of semiconductor supports in related reactions will provide valuable insight into the design of catalysts with improved activity by taking electron–matter interactions into account.

Experimental Section

Synthesis of Pd nanocubes and Pd–TiO_2 hybrid structures: The Pd nanocubes were synthesized according to a previously described protocol.[16] In a typical synthesis, 8.0 mL of an aqueous solution containing poly(vinyl pyrrolidone) (PVP, MW = 55000, Sigma–Aldrich, 856568-100g; 105 mg), L-ascorbic acid (AA, Sigma–Aldrich, A0278-25g; 60 mg), and KBr (300 mg) was heated in a 50 mL three-necked flask for 10 min at 80 °C with magnetic stirring. Subsequently, 3.0 mL of an aqueous solution of potassium palladium(II) chloride ($[K_2PdCl_4]$, Aladdin, 1098844-1g; 63 mg) was added with a pipette, and the reaction mixture was stirred at 80 °C for 3 h. The product was collected by centrifugation and washed three times with deionized water to remove excess PVP. The Pd–TiO_2 hybrid structures were obtained by following the procedure used for the synthesis of Pd nanocubes, but with TiO_2 (Aeroxide, TiO_2-P25; 20 mg) included in the initial aqueous solution (8.0 mL). See the Supporting Information for the characterization of the samples.

Characterization by ultrafast spectroscopy: The ultrafast transient absorption data were recorded on a modified pump–probe spectrometer (ExciPro, CDP) in combination with an amplified femtosecond laser system (Coherent). A schematic illustration of the optical layout (see Figure S10) and the experimental details can be found in the Supporting Information. The samples were dispersed in ethylene glycol for all pump–probe characterizations performed under ambient conditions.

See the Supporting Information for 4-oxo-TMP measurements, glucose oxidation, and computational methods.

Received: November 6, 2013
Revised: January 18, 2014
Published online: February 12, 2014

Keywords: heterogeneous catalysis · oxygen activation · palladium · plasmonics · titania

[1] P. Christopher, H. Xin, S. Linic, *Nat. Chem.* **2011**, *3*, 467 – 472.
[2] X. Xie, Y. Li, Z. Liu, M. Haruta, W. Shen, *Nature* **2009**, *458*, 746 – 749.
[3] L. Kesavan, R. Tiruvalam, M. H. Ab Rahim, M. I. bin Saiman, D. I. Enache, R. L. Jenkins, N. Dimitratos, J. A. Lopez-Sanchez, S. H. Taylor, D. W. Knight, C. J. Kiely, G. J. Hutchings, *Science* **2011**, *331*, 195 – 199.
[4] D. I. Enache, J. K. Edwards, P. Landon, B. Solsona-Espriu, A. F. Carley, A. A. Herzing, M. Watanabe, C. J. Kiely, D. W. Knight, G. J. Hutchings, *Science* **2006**, *311*, 362 – 365.
[5] T. Ishida, N. Kinoshita, H. Okatsu, T. Akita, T. Takei, M. Haruta, *Angew. Chem.* **2008**, *120*, 9405 – 9408; *Angew. Chem. Int. Ed.* **2008**, *47*, 9265 – 9268.
[6] D. Kovalev, M. Fujii, *Adv. Mater.* **2005**, *17*, 2531 – 2544.
[7] J. Wahlen, D. E. De Vos, P. A. Jacob, P. L. Alsters, *Adv. Synth. Catal.* **2004**, *346*, 152 – 164.
[8] R. Vankayala, A. Sagadevan, P. Vijayaraghavan, C.-L. Kuo, K. C. Hwang, *Angew. Chem.* **2011**, *123*, 10828 – 10832; *Angew. Chem. Int. Ed.* **2011**, *50*, 10640 – 10644.
[9] R. Long, K. Mao, X. Ye, W. Yan, Y. Huang, J. Wang, Y. Fu, X. Wang, X. Wu, Y. Xie, Y. Xiong, *J. Am. Chem. Soc.* **2013**, *135*, 3200 – 3207.
[10] J. Yang, D. Wang, H. Han, C. Li, *Acc. Chem. Res.* **2013**, *46*, 1900 – 1909.
[11] A. L. Linsebigler, G. Lu, J. T. Yates, *Chem. Rev.* **1995**, *95*, 735 – 758.
[12] S. A. Wyrzgol, S. Schäfer, S. Lee, B. Lee, M. Di Vece, X. Li, S. Seifert, R. E. Winans, M. Stutzmann, J. A. Lercher, S. Vajda, *Phys. Chem. Chem. Phys.* **2010**, *12*, 5585 – 5595.
[13] C. G. Silva, R. Juárez, T. Marino, R. Molinari, H. García, *J. Am. Chem. Soc.* **2011**, *133*, 595 – 602.
[14] Y. C. Pu, G. Wang, K. D. Chang, Y. Ling, Y. K. Lin, B. C. Fitzmorris, C. M. Liu, X. Lu, Y. Tong, J. Z. Zhang, Y. J. Tsu, Y. Li, *Nano Lett.* **2013**, *13*, 3817 – 3823.
[15] Z. W. Seh, S. Liu, M. Low, S. Y. Zhang, Z. Liu, A. Mlayah, M. Y. Han, *Adv. Mater.* **2012**, *24*, 2310 – 2314.
[16] B. Li, R. Long, X. Zhong, Y. Bai, Z. Zhu, X. Zhang, M. Zhi, J. He, C. Wang, Z.-Y. Li, Y. Xiong, *Small* **2012**, *8*, 1710 – 1716.
[17] R. Konaka, E. Kasahara, W. C. Dunlap, Y. Yamamoto, K. C. Chien, M. Inoue, *Free Radical Biol. Med.* **1999**, *27*, 294 – 300.
[18] J. A. Badwey, M. L. Karnovsky, *Annu. Rev. Biochem.* **1980**, *49*, 695 – 726.
[19] H. Brune, J. Wintterlin, R. J. Behm, G. Ertl, *Phys. Rev. Lett.* **1992**, *68*, 624 – 626.
[20] A. J. Komrowski, J. Z. Sexton, A. C. Kummel, *Phys. Rev. Lett.* **2001**, *87*, 246103.
[21] J. Behler, B. Delley, S. Lorenz, K. Reuter, M. Scheffler, *Phys. Rev. Lett.* **2005**, *94*, 036104.
[22] M. Besson, F. Lahmer, P. Gallezot, P. Fuertes, G. Fleche, *J. Catal.* **1995**, *152*, 116 – 121.
[23] A. Tathod, T. Kane, E. S. Sanil, P. L. Dhepe, *J. Mol. Catal. A* **2013**, DOI: 10.1016/j.molcata.2013.09.014.
[24] L. A. Larew, D. C. Johnson, *J. Electroanal. Chem.* **1989**, *262*, 167 – 182.
[25] M. Z. Luo, R. P. Baldwin, *J. Electroanal. Chem.* **1995**, *387*, 87 – 94.
[26] P. Hannaford, *Femtosecond Laser Spectroscopy*, Springer: New York, **2005**.
[27] G. V. Hartland, *Chem. Rev.* **2011**, *111*, 3858 – 3887.
[28] J. Liu, J. Li, A. Sedhain, J. Lin, H. Jiang, *J. Phys. Chem. C* **2008**, *112*, 17127 – 17132.
[29] Y. Xiong, J. Chen, B. Wiley, Y. Xia, Y. Yin, Z. Y. Li, *Nano Lett.* **2005**, *5*, 1237 – 1242.

